Operation strategy and energy-saving of the solar lighting/heating system through spectral splitting

PLEASE CITE THE PUBLISHED VERSION

https://doi.org/10.1016/j.enbenv.2022.01.002

PUBLISHER

Elsevier

VERSION

VoR (Version of Record)

Energy and Built Environment 4 (2023) 270–280

Contents lists available at ScienceDirect

Energy and Built Environment

journal homepage: http://www.keaipublishing.com/en/journals/energy-and-built-environment/

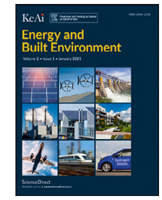

Operation strategy and energy-saving of the solar lighting/heating system through spectral splitting

Chao Shen[a,*], Kaijie Zheng[a], Changyun Ruan[a], Guoquan Lv[a], Mahroo Eftekhari[b]

[a] *School of Architecture, Harbin Institute of Technology, Key Laboratory of Cold Region Urban and Rural Human Settlement Environment Science and Technology, Ministry of Industry and Information Technology, Harbin 15000, China*

[b] *School of Architecture, Building and Civil Engineering, Loughborough University, Loughborough, UK*

ARTICLE INFO

Keywords:
Office building
Energy consumption
Solar lighting/heating
Lighting control strategy
Energy-saving benefits

ABSTRACT

The performance of a solar lighting and heating system (SLHS) based on the spectral splitting effect of nanofluids is presented in this paper. SLHS through nanofluids would split the sunlight spectrum into different wavelength, and then introduce the visible light into the offices for lighting and absorb infrared energy to generate hot water. The Energy Plus software was used to analyze the energy consumption of typical office building located in the city of Harbin in China coupled with SLHS. Based on the simulation results two lighting zones were identified in the offices and the optimal lighting control strategy was developed for a full year. The performance models of SLHS with different light-receiving areas of 10 m^2 and 40 m^2 were simulated and validated using the existing experimental data. The overall energy-saving of the offices over a full year were analyzed using the validated model. Results demonstrated that for SLHS with the area of 40 m^2, the rate of the energy saving in the offices due to lighting and hot water systems were 58.9%, and 19.3%, respectively. The system also had the additional benefit of reducing the cooling load of the air conditioning system during summer period together with improving the quality of the indoor environment resulting in better health and productivity of the occupants.

1. Introduction

It is a well-known fact that using solar energy as a clean energy source for building energy supply will greatly reduce the consumption of other energy sources in buildings [1]. Liang [2] presented an active solar building façade system. The system can make full use of solar energy to produce hot water and electricity. Kumar [3] showed the effectiveness of an adaptive neuro-fuzzy inference system for controlling the lighting system through outdoor climate parameters. Taking climate data as the standard data input, for solar PV module and daylight-artificial integrated scheme power analysis. The system powered by a renewable source and daylight is appropriately utilized in the lighting system. However, the actual use of solar energy has the disadvantages of low energy conversion efficiency and high operating costs [4].

As a crucial part of the built environment, the light environment directly affects the physical and mental health of the occupants and their productivity. Compared with single-spectrum artificial light sources, natural light has the benefits of relieving visual fatigue, improving the moods of the occupants and their productivity [5]. In cold regions, people are spending more time indoors, and the lack of sunlight aggravate the incidence of related diseases known as winter blues, particularly in the elderly population [6]. Light environmental factors such as illuminance, color temperature, and spatial distribution affect the human body but also through non-visual channels influence the circadian rhythm of the body, such as sleep quality and mood. It has been reported that blue-rich white light has a more pronounced effect on energetic awakening in the morning and midday, and that people have the same sensitivity to color temperature throughout the workday [7]. Therefore, in office buildings, the introduction of natural light lighting is important for improving productivity as well as protecting occupants' health.

In the late 1990s, Choi [8] proposed the concept of nanofluids to solve the problem of low thermal conductivity of high-efficiency heat transfer fluids required by industry. Wang [9] pointed out that nanofluids have unique optical properties that can absorb and scatter incident light. Related research pointed out that the metal nanofluids has the phenomenon of selective absorption of the fluid for the spectrum, which is manifested as the blue and red shift of the absorption band, and the strong absorption of the broadband [10]. In addition, changes in the type and size of nanoparticles can also affect the radiation characteristics of the nanofluids working medium. The nanofluids can selectively absorb and transmit the incident light of a specific wavelength band [11].

The excellent heat transfer performance of nanofluids had been verified by experiments. Kandeal [12] uses nanofluids as the cooling liquid

* Corresponding author.
E-mail address: chaoshen@hit.edu.cn (C. Shen).

https://doi.org/10.1016/j.enbenv.2022.01.002
Received 12 November 2021; Received in revised form 4 January 2022; Accepted 4 January 2022
Available online 11 January 2022

Nomenclature

Abbreviations

G_0	The intensity of direct solar radiation (W/m^2)
E_0	The intensity of direct sunlight (lux)
Q_0	The heat input to the system (W)
ϕ_0	The luminous flux input to the system (lm)
Q_1	The heat output from the system (W)
ϕ_1	The luminous flux output from the system (lm)
A_{lens}	The area of Finer Lens (m2)
c	The specific heat capacity of nanofluid $(\mathrm{kJ/kg \cdot K})$
V	The Circulating flow rate of nanofluid (L/h)
ρ	The density of nanofluid $(\mathrm{kg/m^3})$
t_1	The Outlet temperature of nanofluid (°C)
t_0	The inlet temperature of nanofluid (°C)
η_i	The transmission efficiency of visible light
η_j	The thermal efficiency of SLHS
Q_h	The design heat consumption per hour for heating hot water (kJ/h)
m	The number of water-consumption based on the number of people or beds
q_r	The fixed hot water consumption $[\mathrm{L/(person \cdot day)}]$
t_r	The temperature of hot water (°C)
C	The specific heat capacity of water $[\mathrm{kJ/(kg \cdot ^\circ C)}]$
t_1	The temperature of cold water (°C)
ρ_r	The density of hot water $(\mathrm{kg/L})$
T	The daily use time (h)
C_γ	The heat loss coefficient of the hot water supply system
K_h	The hourly variation coefficient

for photovoltaic panels and found that the surface temperature reduction can reach 16 °C with enhancement in electrical efficiency up to 50% compared to conventional uncooled PV panels. MimiElsaid [13] confirmed that hybrid nanofluids have better heat transfer performance than single nanofluids. Essa [14], B.Abdelaziz [15] and W.Sharshir [16,17] found that nanofluids can improve the productivity and thermal efficiency of solar stills through experiments, thereby saving operating costs. Related scholars have also carried out related researches on the optimization of nanofluids performance. Tielke [18] verified that the thermal conductivity of nanofluids is directly proportional to the concentration and temperature through experiments, and found that the thermal conductivity of some nanofluids is related to particle size. Nanofluids are widely used in the field of solar energy utilization due to their good thermal properties. Torres [19] used low sonication energy values to prepare a more stable nanofluids, and its heat transfer performance was also improved.

In the evaluation of system energy efficiency, building energy consumption is a quite important indicator [20]. Building energy consumption simulation will help people formulate scientific operation strategy. Rajeev [21] studied the strategic control and cost optimization of building thermal storage technology, by constructing a large office building with Energy Plus, and designed the operation strategy of coupling building thermal storage technology and coping with high and low electricity peak price system. B.Abdelaziz [22] installed a Heat Pipe Heat Exchanger (HPHE) between the fresh air and return air streams in the air-condition to cool the fresh air before entering the air handing unit. Through experimental verification, this measure saves a lot of building energy consumption, which is proved to be effective.

The SLHS system can take advantage of solar radiation energy to reduce building energy consumption. In the mathematical model and experiment, the photothermal efficiency of the system has been quantitatively calculated [23]. But the energy-saving situation and operation strategy of this system in a specific building have not been developed yet. In this research, Energy Plus was used to simulate and calculate the energy consumption of the system in an office building. Based on the simulation results, the operating strategy was given. This article mainly introduced the SLHS system and building model in Chapter 2. Chapter 3 introduced the detailed situation of model establishment and energy consumption simulation. Chapter 4 mentioned the lighting control strategy. The specific energy-saving benefits of the system and cost analysis were introduced in Chapter 5. The research used simulation for the first time to verify the feasibility of nanofluid photothermal separation technology in building energy saving. The research results in this article can inspire more scientific researchers to explore the application of nanofluids.

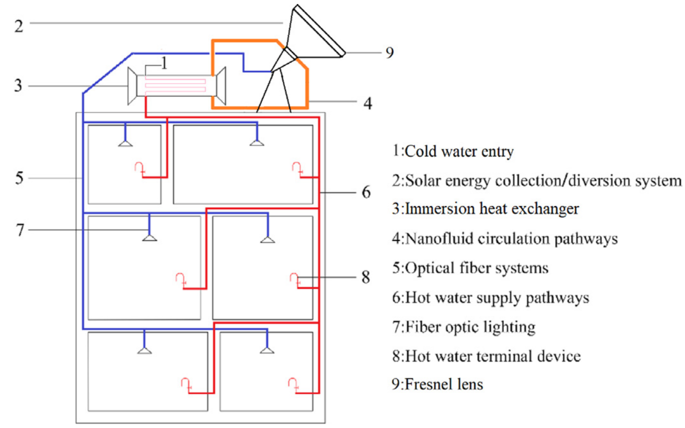

Fig. 1. SLHS System operation principles.

2. The description of SLHS and building

2.1. System principles

The SLHS is mainly divided into three parts: sunlight receiving end, light and heat transmission channel, and an output end. The sunlight receiving end adopts the concentrating optical element with nanofluidic wavelength splitting device to converge and shunt the sunlight for efficient bi-directional utilization.

The photothermal transmission channel ensures the feasibility of energy from reception to utilization, which mainly includes optical fiber system and nano-fluid pipeline. After the sunlight passes through the specific modulated nanofluid, the light and heat energy are the output in a certain ratio. Most of the absorbed infrared rays are converted into heat, which is then introduced into the building interior by using immersion heat exchanger through the nano-fluid circulation system to provide domestic hot water inside the building. The transmitted visible light is fed through the fiber optic system and is supplied into the interior to supplement building lighting [24]. This will also solve the problems of fiber optic thermal protection and receiver and beam convergence coupling [25].

The output end mainly includes the domestic hot water utilization system and fiber optic lighting equipment, which makes full use of the two parts of the diverted energy indoors and reduces the overall energy consumption of the building. Fig. 1 shows the specific equipment situation.

2.2. Energy delivery

Fig. 2 shows the SLHS energy delivery operation, which help to understand the flow sequence and quantity of the energy. The radiant energy emitted by the sun is collected by the solar energy collector to harvest high density energy. The concentrated solar radiation irradiates the nanofluids container. The nanofluids inside the container carry this solar radiation energy and use this for heating domestic hot water. At

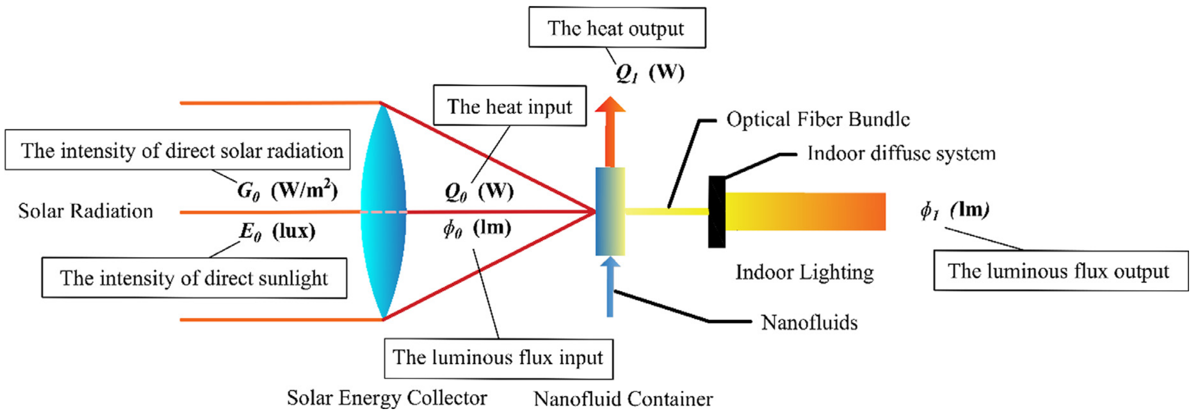

Fig. 2. SLHS system Energy delivery process.

the same time, the visible wavelength of solar radiation is transmitted into the pre-arranged optical fiber bundle by the nanofluid container and generates indoor lighting. The infrared energy and visible light in solar radiation are reasonably decomposed and utilized.

It can be seen from the Fig. 2 that the total solar luminous flux input to the SLHS system can be calculated by Eq. (1) [26]:

$$\phi_0 = E_0 A_{lens} \quad (1)$$

The transmission efficiency of visible light can be calculated by Eq. (2):

$$\eta_i = \frac{\phi_1}{\phi_0} \quad (2)$$

Similarly, the solar radiation energy input to the system can be estimated by Eq. (3) [27]:

$$Q_0 = G_0 A_{lens} \quad (3)$$

The heat absorbed by the system can be calculated by Eq. (4):

$$Q_1 = c \cdot \rho \cdot V \cdot (t_1 - t_0) \quad (4)$$

Therefore, the thermal efficiency of SLHS is given by using Eq. (5):

$$\eta_j = \frac{Q_1}{Q_0} \quad (5)$$

2.3. Parameter setting

To make this research general and applicable to most buildings in Chinese severe cold climate regions, the construction of a standardized building was used. All parameters of this building were defined using relevant design codes. The selected building is a four-story office building in Harbin City, Heilongjiang Province, south facing, with a building area of 2054.8 m^2. The window-to-wall ratio which meets the energy-saving requirements of the Energy Conservation Design Standards for Residential Buildings in Severe Cold and Cold Regions [28] for the different facades are North 21.61%; South 21.11%; East 3.77%; West 0.

This building is a complex site consisting of offices, conference offices, restrooms, toilets, stairwells, and other functional areas with a considerable demand for lighting and hot water supply, which makes this the most suitable research scenario. Energy Plus was used to simulate the energy consumption of the building and investigate the SLHS operation strategy together with the energy saving benefits.

The building model was set up using Sketch Up and Open Studio plug-ins based on the building plan (as shown in Fig. 3, and the IDF file was exported and imported into Energy Plus software, where detailed information on internal and external factors and relevant building materials were used for simulation of the building energy consumption.

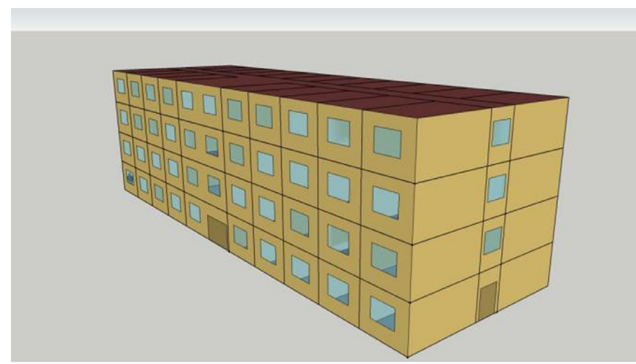

Fig. 3. Office building model shown in Sketch Up.

SLHS not only can provide domestic hot water and lighting but also improves the quality of indoor lighting. Therefore, it is necessary to pre-calculate and set the building hot water parameters. The following calculation process mainly applies to the "Design Standard for Building Water Supply and Drainage". According to the calculation requirements in the code, the hourly design of heat consumption of the whole day for centralized hot water supply system in office buildings could be calculated using Eq. (6). Overall, the design heat consumption per hour is 62,204.97 kJ/h for heating the hot water.

$$Q_h = K_h \frac{mq_r C(t_r - t_1)\rho_r}{T} C_\gamma \quad (6)$$

To make the simulation results general, the envelope enclosure, internal disturbance information, air conditioning system all included in the simulation based on the requirements of the code for cold regions. The weather data for the simulations were adopted from the Chinese Standard Weather Data (CSWD) for Harbin city, whose annual outdoor dry bulb temperature and annual direct solar radiation graphs are shown above in Figs. 4 and 5, respectively.

3. Modeling and validation

January 20 and July 21 were selected as typical winter and summer days, and two typical offices with the same area, and function but different orientation were randomly selected for analysis. The indoor dry bulb temperature results are shown in Figs. 6 and 7 below.

Harbin is in a severe cold region under the climate partition of China, with four distinct seasons, and the calculated outdoor temperature during winter is as low as −24.2 °C, while the calculated outdoor temperature for the summer is as high as 30.7 °C. The temperature difference between winter and summer is very considerable [29]. From the above

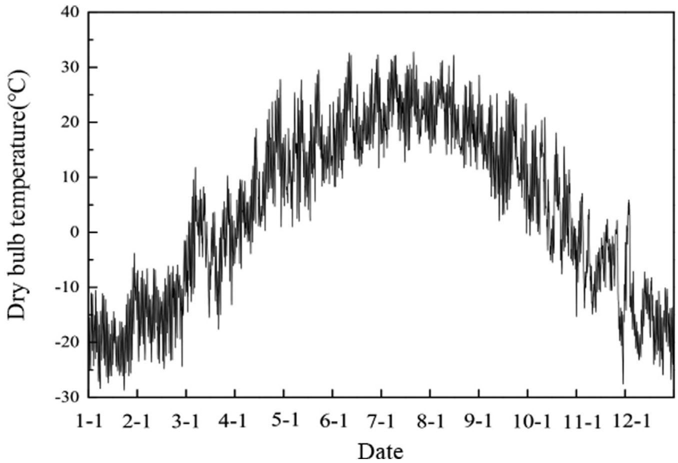

Fig. 4. Harbin annual outdoor hourly dry bulb temperature.

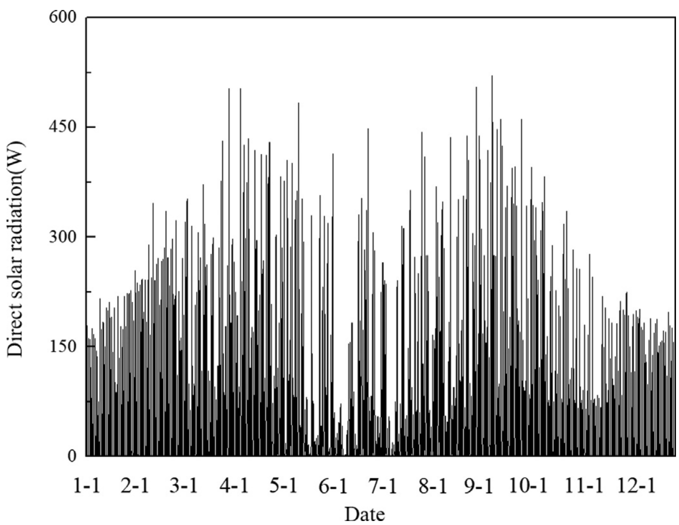

Fig. 5. Harbin annual hourly direct solar radiation.

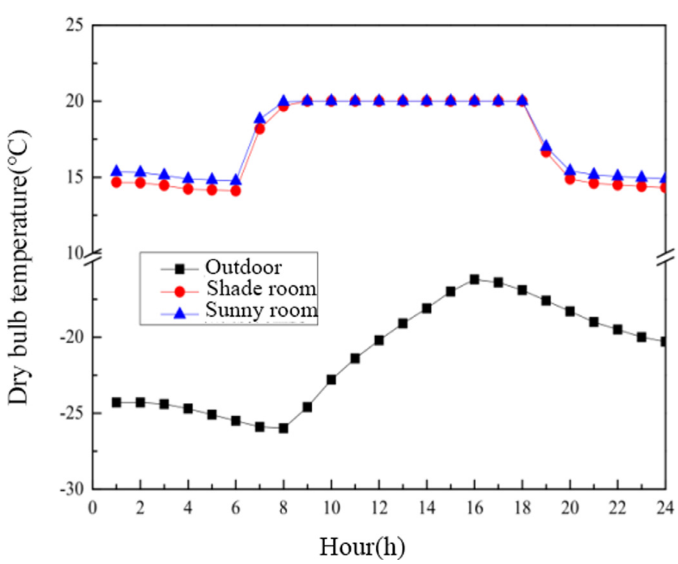

Fig. 6. Office room indoor and outdoor temperature in winter.

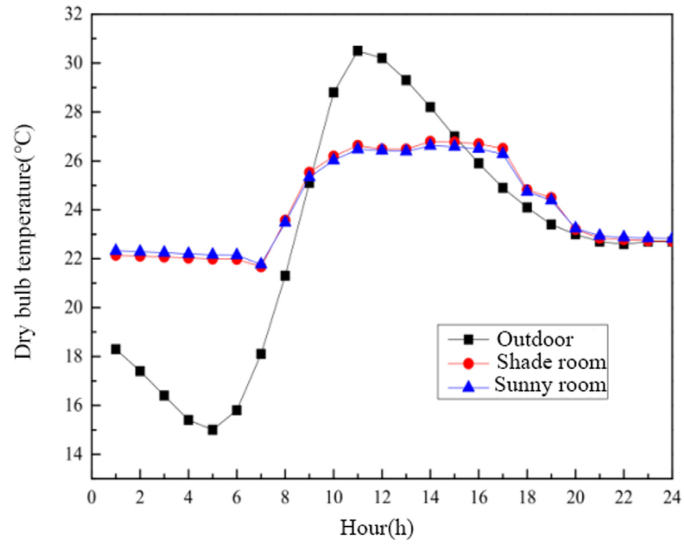

Fig. 7. Office room indoor and outdoor temperature in summer.

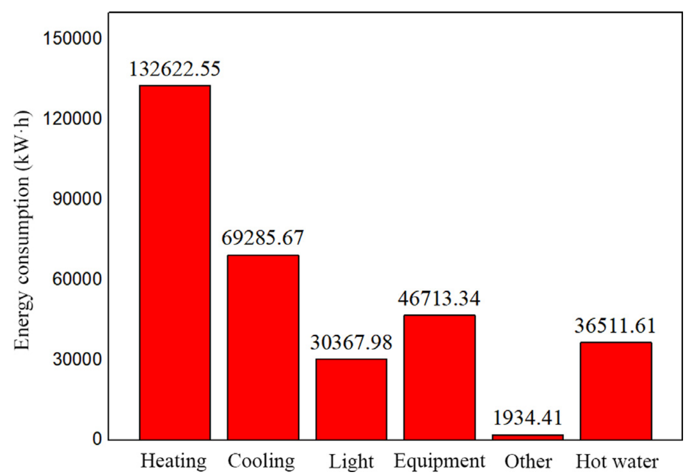

Fig. 8. Building energy consumption.

figure, the outdoor dry bulb temperature roughly shows a cosine function waveform variation [30], while the indoor temperature is always maintained within the relative comfort temperature range due to the regulation of the heating and cooling systems.

As shown in Fig. 7, the lowest value of the outdoor dry bulb temperature recorded is at 5 a.m. in the morning, however the office temperature is not at its lowest due to the thermal inertia of the building materials. The air conditioning is scheduled to switch on at 6 a.m. in the morning. In addition, when the air conditioner is not running, the temperature of the office on the sunny side is about 0.5 °C higher than that of the office on the shaded side, both during summer and winter periods, which is mainly due to solar radiation. From the above results, the simulated air-conditioning system can meet the comfort requirements.

The main energy consumptions in the office buildings are heating, cooling, hot water, lighting, and equipment loads. The simulated energy consumption in the building is shown below in Fig. 8.

The HVAC software of Tianzheng was used to calculate the cooling and heating loads, and the results were compared to the Energy Plus cooling and heating loads for validation. The results of the building design load calculations are shown below in Table 1.

The cooling and heating loads obtained from the design calculations are converted into annual energy consumption values based on 8 h/day weekdays operation only over 6 months of heating in winter

Table 1
Design value of building cooling and heating load from HVAC software of Tianzheng.

Floor	1	2	3	4	Sum
Heating load(W) (((W)	49,238	30,089	27,684	27,500	134,511
Cooling load(W) (W)	50,022	50,022	50,022	50,022	200,090

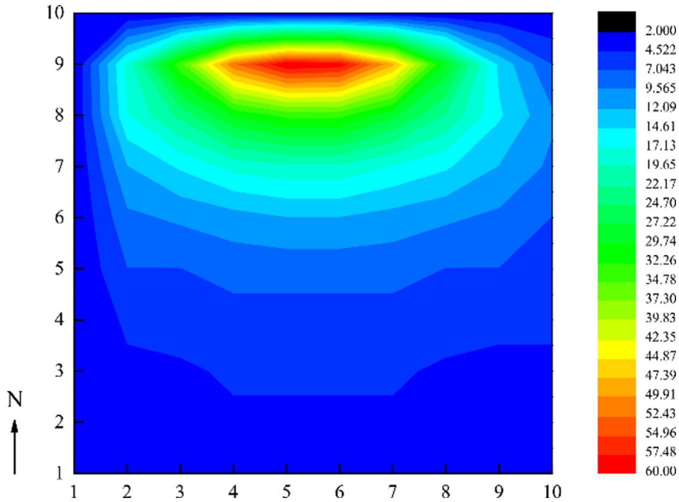

Fig. 9. 8:00 on January 20th, the distribution of light intensity in the shaded office (lx).

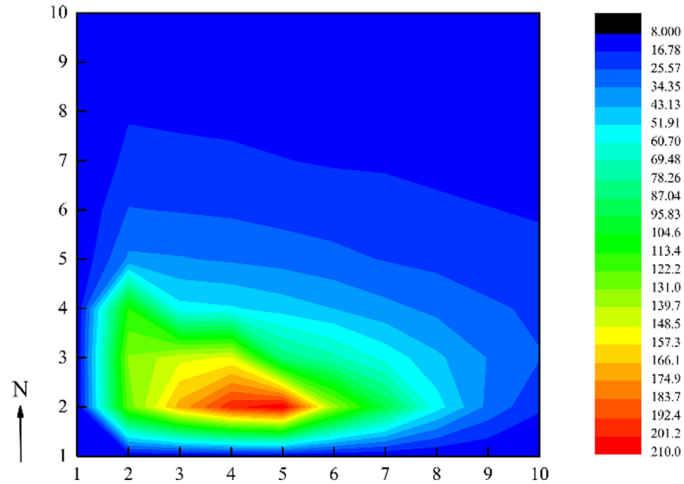

Fig. 10. 8:00 on January 20th, the distribution of light intensity in the sunny office (lx).

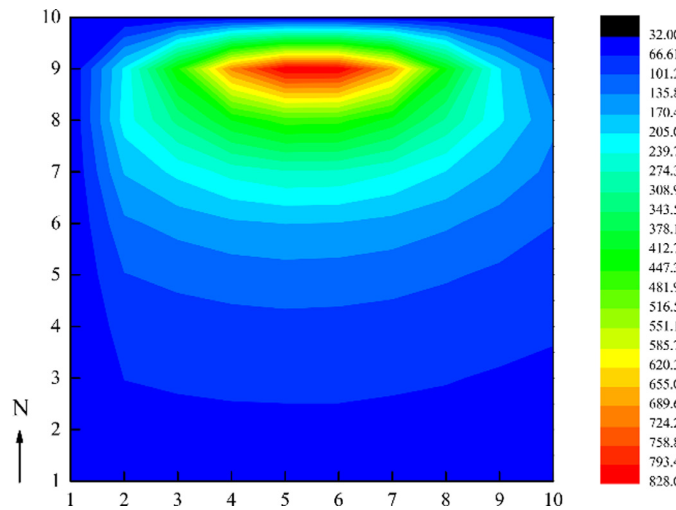

Fig. 11. 14:00 on January 20th, the distribution of light intensity in the shaded office (lx).

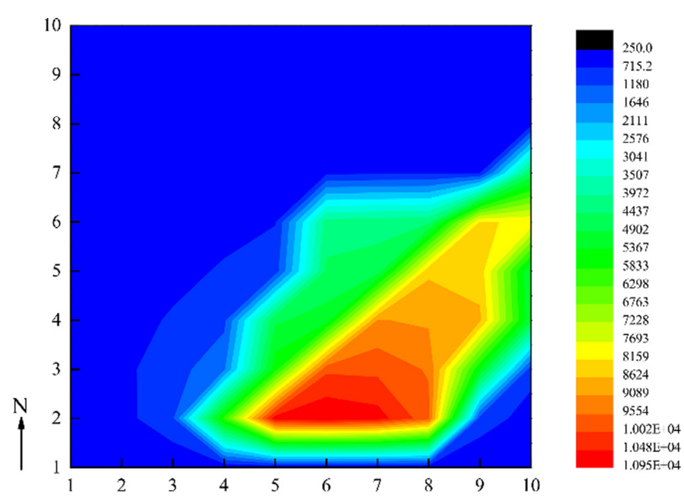

Fig. 12. 14:00 on January 20th, the distribution of light intensity in the sunny office (lx).

and 2 months of cooling in summer. Therefore the annual heating and cooling energy consumptions are 138,354.17 kW h and 68,602.29 kW h, respectively. The difference between the design and simulated heating and cooling energy consumption is 4.14% and 0.95%, respectively. Both values are within 5%, which proves that the building is reasonably simulated [31], and the results are valid for a wide range of application in the cold region.

4. Lighting zones division and system energy-saving strategy

The lighting demand of office buildings is mainly during the day. At the same time, due to the shading devices, as the external natural light radiation increases there is a greater demand for indoor lighting. This is reflected in a positive correlation between the indoor lighting demand of office buildings and the outdoor light intensity [32]. The light distribution in the office is very uneven due to the depth of the office. Therefore, the use of localized lighting in office buildings will have a great impact on energy consumption [33]. This study will investigate different lighting strategy and personalized lighting systems suitable for SLHS by partitioning the lighting conditions inside the offices.

4.1. Division of lighting zones

January 20th and July 20th were selected as typical winter and summer days. Two offices one in a shaded and one in sunny locations were randomly selected for this study. The depth of the office is 5.18 m, the width is 3.4 m, and the total area is 17.6 m^2. The Day Lighting Control and the Illuminance Map is located at the height of 0.75 m in the simulated office. The light intensity distribution of both offices is shown in Figs. 9–16.

The horizontal axis, denoted as $x = 0$–10; and the longitudinal direction, denoted as $y = 0$–9 mark 11 and 10 equidistant points, respectively. These points are extended in a straight line perpendicular to the wall, and then the straight lines intersect to form 110 points altogether in the office, which are used as simulated photosensitive points as shown in Fig. 17. As the outdoor radiation changes, the light intensity received

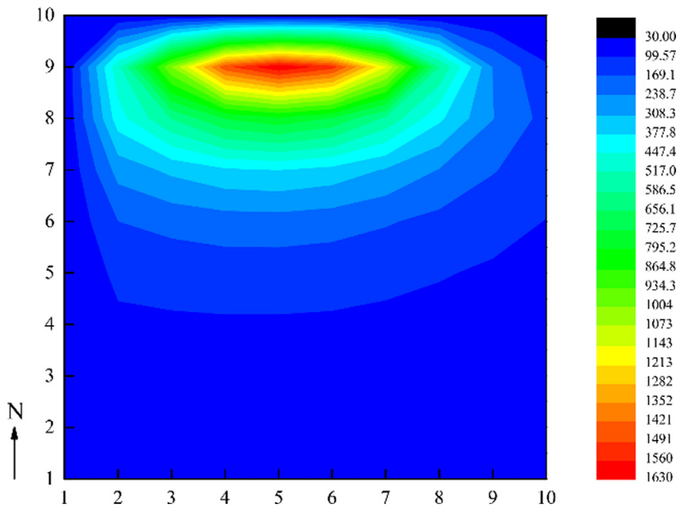

Fig. 13. 8:00 on July 20th, the distribution of light intensity in the shaded office (lx).

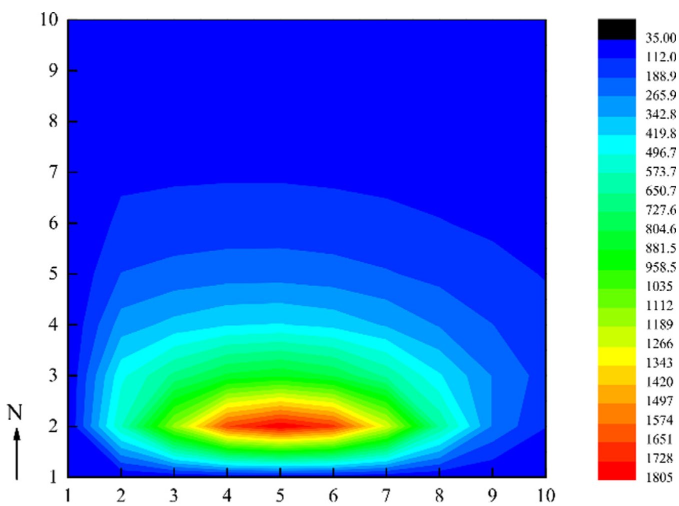

Fig. 14. 8:00 on July 20th, the distribution of light intensity in the sunny office (lx).

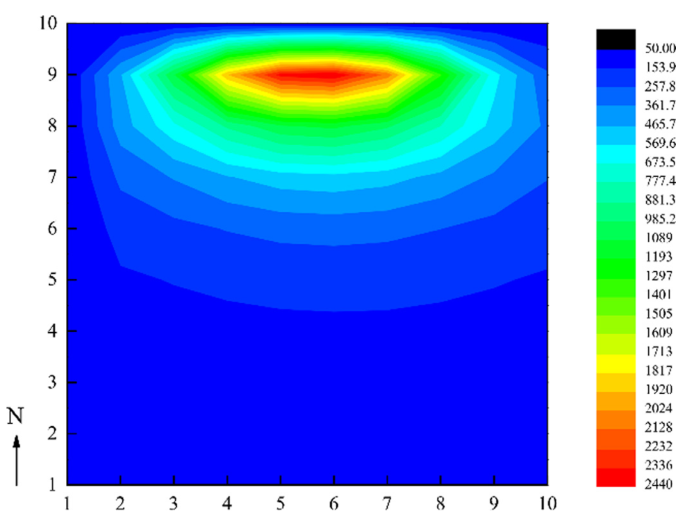

Fig. 15. 14:00 on July 20th, the distribution of light intensity in the shaded office (lx).

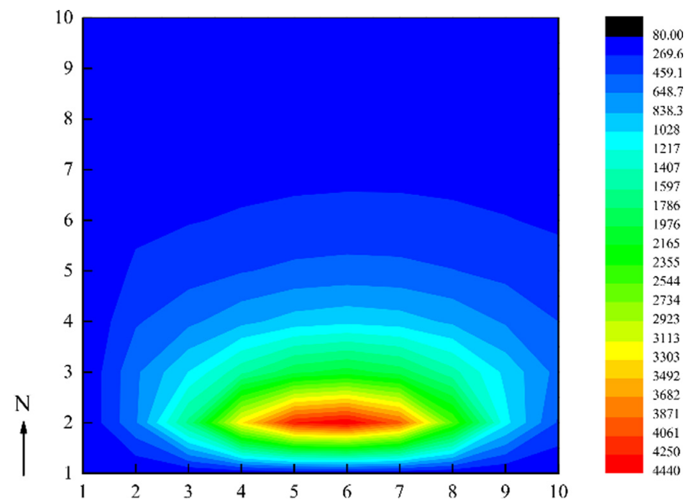

Fig. 16. 14:00 on July 20th, the distribution of light intensity in the sunny office (lx).

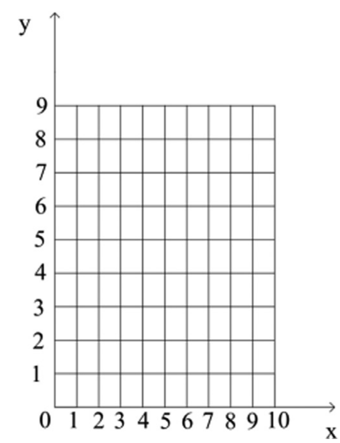

Fig. 17. Schematic diagram of 2-D coordinate distribution of indoor photosensitive points.

by the photosensitive spot also changes constantly which forms the basis for dividing the lighting partition, and the control strategy.

Figs.18 and 19 show the depth as the independent variable, and the average light intensity of the typical days for the four seasons of the shaded and sunny offices as the dependent variable. As can be seen from the above Fig. 18, when the office depth is between x = 0~7, the office has an average light intensity of less than 200 lx throughout the year; and when the office depth is around x = 7~9, the office lighting condition is significantly improved, and the illuminance is greater than 200 lux. At the depth of x = 9, the light intensity is negligible mainly since photosensitive spot is close to the edge of the window. Therefore, using the straight-line at the depth of x = 7 as the critical line, the shaded office's lighting is divided into zone I and zone II with areas of 3.9 m^2, and 13.7 m^2, respectively (see Fig. 20). Similarly for the sunny office Fig. 19, the dividing critical line in the office is at the depth of x = 4 with area of zones I and II as 7.8 m^2 and 9.8 m^2, respectively as shown in Fig. 21.

4.2. Lighting control strategy

To further improve the energy effectiveness of the SLHS, it is also necessary to develop lighting strategy for different lighting zones discussed above. The principle of setting strategy mainly includes the following three points:

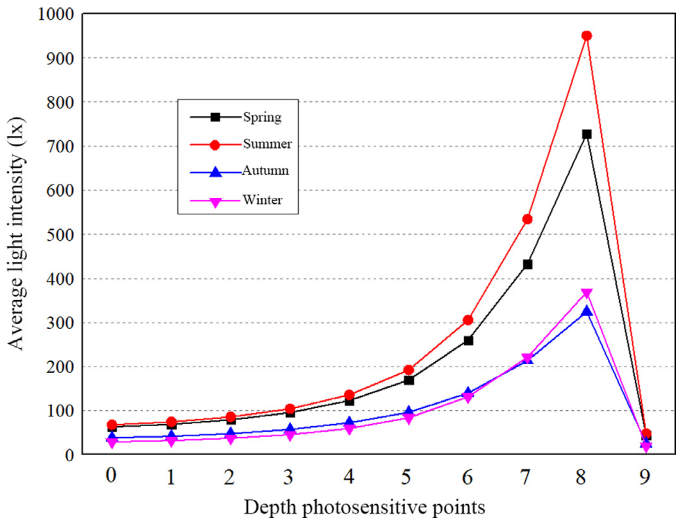

Fig. 18. A graph of the average light intensity changes at each depth of the typical day in the four seasons of the shaded office.

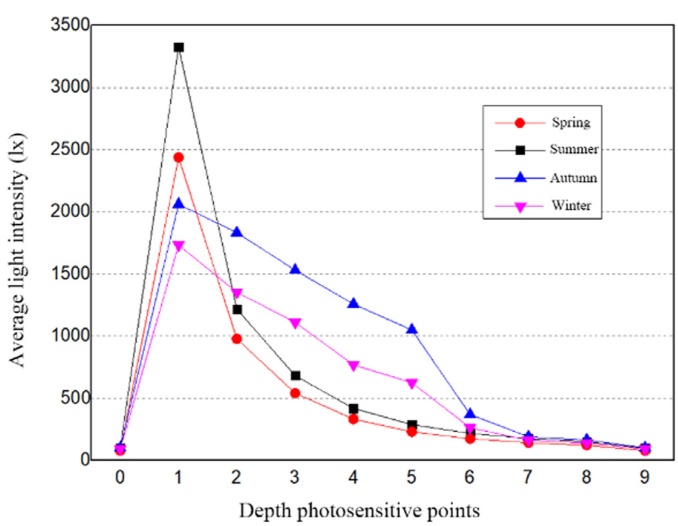

Fig. 19. A graph of the average light intensity changes at each depth of the typical day in the four seasons of the sunny office.

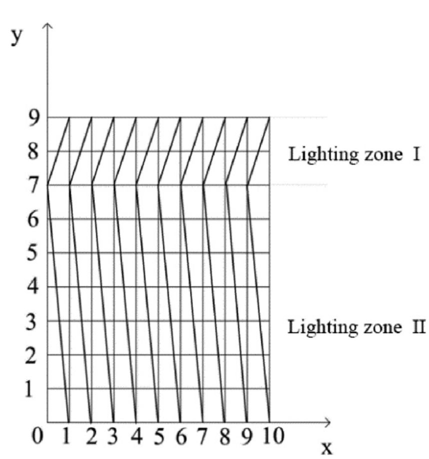

Fig. 20. Lighting zone division of shaded office.

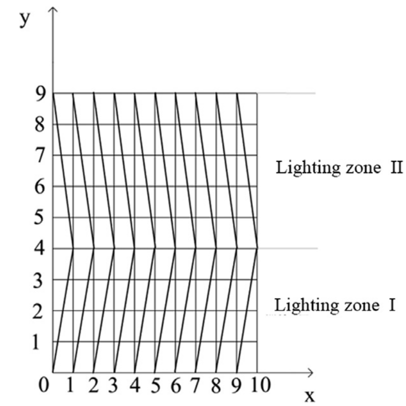

Fig. 21. Lighting zone division of sunny office.

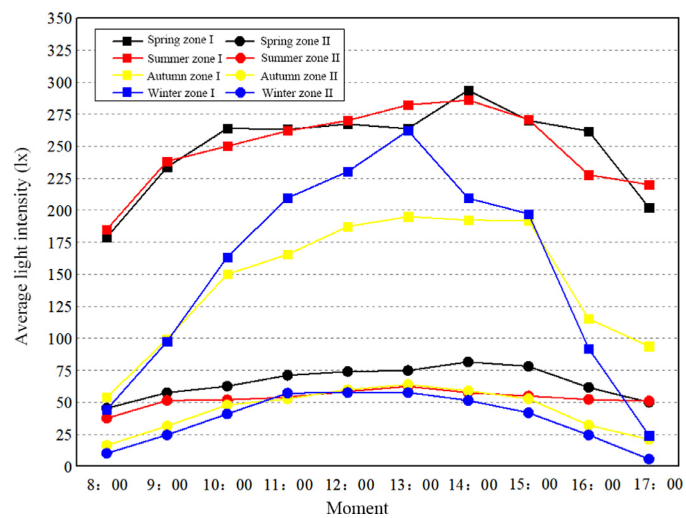

Fig. 22. The average illuminance changes of each lighting zone in the shaded office during four seasons.

(1) The lighting level at desk level of 0.75 m has to meet the standard illuminance of 400 lux throughout the year;
(2) The indoor lighting intensity must be satisfied in all the offices in particular the office in shaded locations;
(3) Energy consumptions will be simulated based on the assumptions that the lighting levels meet the comfort requirements of the occupants.

Based on these above criteria the annual indoor hourly illumination intensity distribution for both offices at desk level during working hours of 8:00 a.m. –17:00 p.m., for different seasons and the two zones were simulated and are shown in Figs. 22 and 23.

It can be seen from the above figures that average illuminance in zone I for both offices are much higher than in zone II. The change of lighting illumination in zone II is relatively constant, which demonstrates that the change of outdoor natural light radiation has hardly any effect on the lighting zone II.

Based on the Architectural Lighting Design Standards [34] recommendation the maintained illuminance required at the desk level of 0.75 m is 400 lux. Therefore, to achieve this illuminance using additional localized lighting is required in both offices. A control strategy was developed to predict the% of the on-time of the additional localized lighting in offices during different seasons and the results are shown in Tables 2 and 3.

In the sunny office in contrast to the shaded office, due to bright lights (see Fig. 23), shading strategies are required to maintain occu-

Table 2
Control strategy for localized light% on-time period in shaded office.

Time	Spring Zone I	Zone II	Summer Zone I	Zone II	Autumn Zone I	Zone II	Winter Zone I	Zone II
8:00	0.55	0.89	0.54	0.91	0.86	0.96	0.89	0.97
9:00	0.42	0.86	0.40	0.87	0.75	0.92	0.76	0.94
10:00	0.34	0.84	0.38	0.87	0.63	0.88	0.59	0.90
11:00	0.34	0.82	0.34	0.86	0.59	0.87	0.48	0.86
12:00	0.33	0.81	0.33	0.85	0.53	0.85	0.42	0.86
13:00	0.34	0.81	0.29	0.84	0.51	0.84	0.34	0.86
14:00	0.27	0.80	0.29	0.86	0.52	0.85	0.48	0.87
15:00	0.33	0.80	0.32	0.86	0.52	0.87	0.51	0.90
16:00	0.35	0.85	0.43	0.87	0.71	0.92	0.77	0.94
17:00	0.50	0.88	0.45	0.87	0.77	0.95	0.94	0.99

Table 3
Control strategy for localised light turn-on degree in sunny office.

Time	Spring Zone I	Zone II	Summer Zone I	Zone II	Autumn Zone I	Zone II	Winter Zone I	Zone II
8:00	0	0.78	0	0.63	0.20	0.86	0.67	0.92
9:00	0.5	0.63	0.5	0.29	0.5	0.62	0	0.73
10:00	0.5	0.55	0.5	0.25	0.5	0.29	0.5	0.44
11:00	0.5	0.33	0.5	0	0.5	0.26	0.5	0
12:00	0.5	0.26	0.5	0	0.5	0.07	0.5	0
13:00	0.5	0.24	0.5	0	0.5	0	0.5	0
14:00	0.5	0.25	0.5	0	0.5	0.20	0.5	0.25
15:00	0.5	0.52	0.5	0.03	0.5	0.44	0.5	0.41
16:00	0	0.66	0.5	0.32	0	0.76	0	0.77
17:00	0.20	0.82	0.5	0.60	0.60	0.91	0.85	0.97

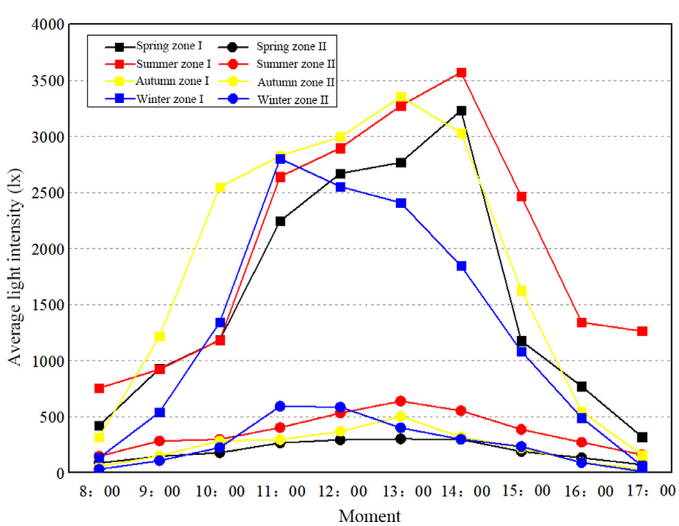

Fig. 23. The average illuminance changes of each lighting zone in the sunny office during four seasons.

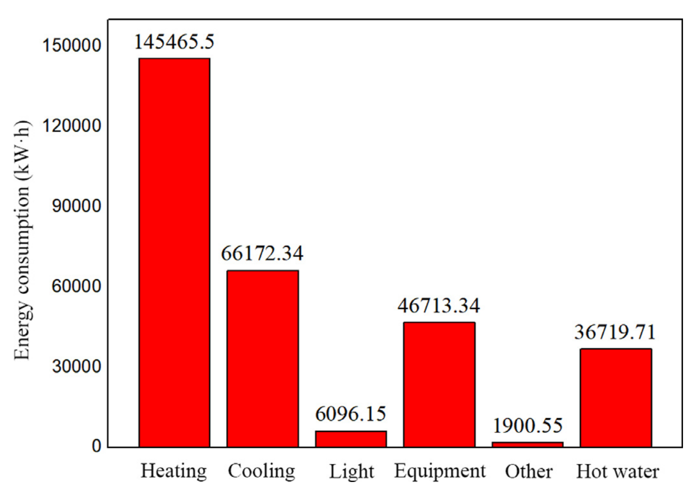

Fig. 24. Building energy consumption after implementing the lighting strategy.

pants' comfort. The following criteria for shading based on simulation results are developed:

(1) Shading devices to be used when the average illuminance is higher than 800 lx, and the turn-on degree of localized lighting is 0.5 or below;
(2) For average illuminance between 400 lx and 800 lx inside the office, there is no need for shading devices or use of artificial light.

4.3. Energy saving of the lighting strategies

Based on the above optimized lighting strategies and modifying the power of LED localized lighting to 3.3 W/m^2, simulated energy consumptions are presented in Fig. 24.

Compared with Fig. 8, the lighting energy consumption (see Fig. 24) of the building is reduced by nearly 80% due to the application of localized lighting strategies and use of LED lighting, which greatly reduces the operation energy cost of the office building.

From Fig. 24 it can also be seen that by using these lighting measures the air condition cooling energy consumption also decreased by 4.49% at the same time.

Table 4

5. Analysis of actual energy saving benefit of the system

The main source of energy consumption in office building are lighting, heating, cooling, and hot water. The SLHS not only reduces the lighting energy demand but also as discussed earlier on it also provides hot water in the buildings. Based on experimental data and mathemati-

Table 4
The specific costs and expected revenues of the SLHS.

Area	Cost (RMB) Fresnel lens	Other costs	Total	Revenues (RMB/year) Lighting	Heat	Total	Payback Period (year)
10 m^2	4500	4000	8500	1072	1412	2484	3.42
40 m^2	18,000	10,000	28,000	2921	5648	8569	3.27

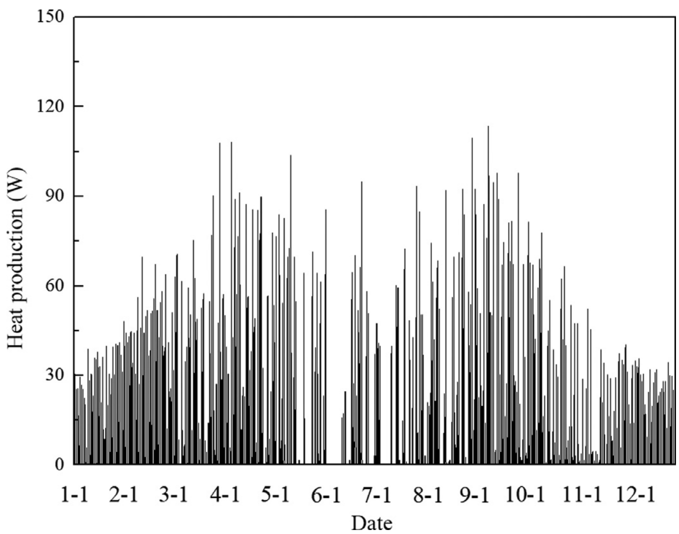

Fig. 25. The hourly heat production per square meter of light-receiving area throughout the year.

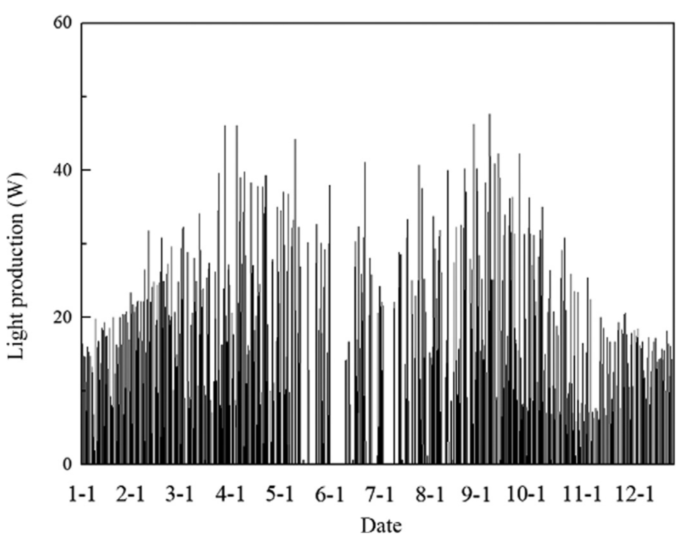

Fig. 26. The hourly amount of natural light input per square meter of light-receiving area throughout the year.

cal models, the relationship between system efficiency and direct solar radiation intensity and outdoor temperature can be analyzed.

Through many experimental studies [23,35], it is found that there is a relationship between the direct solar intensity radiation and the outdoor dry bulb temperature in the photothermal output efficiency of SLHS. Through the data regression calculation, the quantitative relationship is developed for this research.

The meteorological data of Harbin are used in the model to obtain the hourly heat/light production per square meter of the light-receiving area, as shown below in the Figs. 25 and 26.

It can be seen from these above figures that the heat/light production of SLHS is roughly positively correlated with the variation of the direct

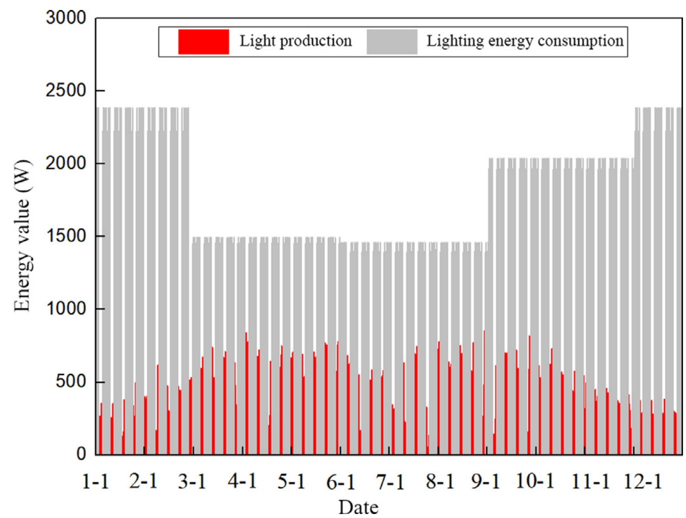

Fig. 27. Hourly comparison chart of light production and building lighting energy consumption of 10 m^2 light-receiving area.

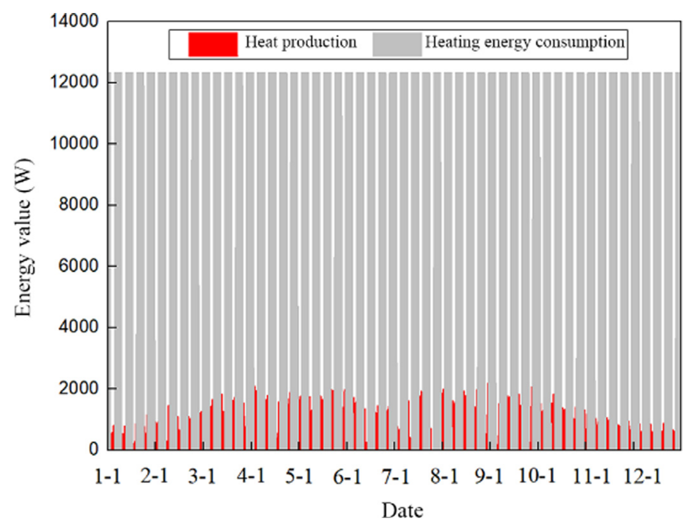

Fig. 28. Hourly comparison chart of heat production from 10 m^2 light-receiving area and energy consumption of building hot water system.

solar radiation. In addition, it is also related to the light-receiving area of SLHS. The energy saving resulted from different light-receiving areas of 10 m^2 and 40 m^2 of the SLHS are simulated and analyzed.

5.1. Energy saving of the system under different light-receiving areas

The roof area of the simulated office building is 513.7 m^2 therefore the light-receiving areas of 10 m^2 and 40 m^2 for SLHS are investigated.

The hourly light and heat production and the actual hourly energy consumption of the building are shown in Figs. 27–30.

From the above graphs for areas of 10 m^2 and 40 m^2, the annual light production of SLHS is 804 kW•h and 2190.62 kW•h, respectively. According to the ratio of light efficiency between natural light and LED

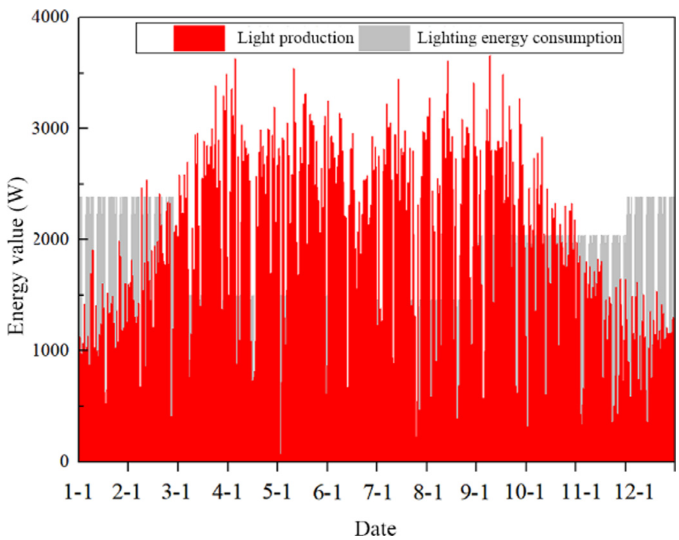

Fig. 29. Hourly comparison chart of light production and building lighting energy consumption of 40 m^2 light-receiving area.

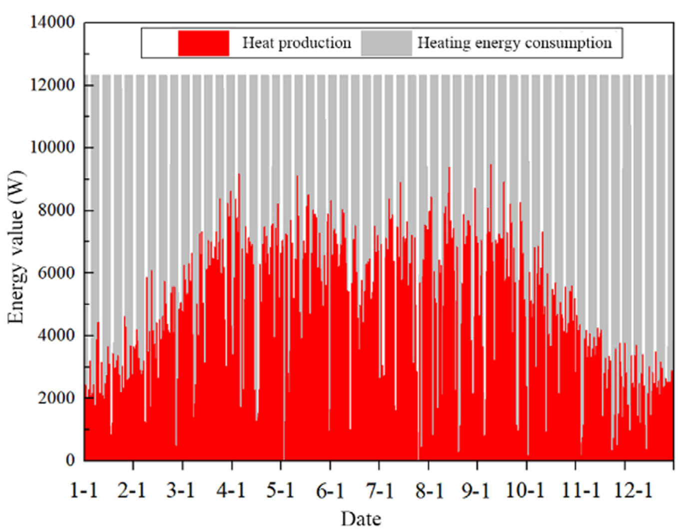

Fig. 30. Hourly comparison chart of heat production from 40 m^2 light-receiving area and energy consumption of building hot water system.

lamps (5:3) [36,37], the energy consumption of natural light is replaced with the energy consumption of LED lamps in the same proportion. The required supplementary lighting power consumption is 4885.11 kW h and 2506.68 kW h. The lighting energy-saving therefore are calculated to be 19.87% and 58.9%.

It can be seen from Fig. 30 that although the heat provided by SLHS could not meet the actual demand for the building, it has significantly reduced the overall electricity consumption. Through calculation, when the light-receiving area is 10 m^2 and 40 m^2, the annual heat production of the system is 1764.94 kW h and 7059.58k kW h, and the supplementary power consumption of the hot water system is 34,799.42 kW h and 29,504.79 kW h, respectively. The energy saving in heat production are 4.82% and 19.3%, respectively.

According to the quantitative calculation of the building area of 2054.8 m^2, the system can provide the lighting demand of 30.46 m^2 of the building area and the hot water demand of 9.92 m^2 of the building area per square meter of light-receiving area.

5.2. Energy saving of air conditioning system during summer

The cooling load of the air conditioning system during the summer includes the façade and internal heat gains. The latter includes indoor electrical equipment, such as lighting and personnel computers. Since in this research the lighting is replaced by natural lighting, the heat emitted by the lighting system is reduced, which in turns reduces the cooling demand.

The results show that the overall total energy consumption of the office building is reduced from 66,172.34 kW h to 65,429.5 kW h during the cooling season in Harbin, with a decrease ratio of 1.12% for light-receiving area of 40 m^2. The results show that SLHS not only reduces lighting and hot water demand but also reduces the cooling load on the air conditioning system.

5.3. The economic analysis

Economic analysis is necessary to be studied to improve the promotion possibilities of the SLHS. The following will show the specific costs and expected revenues of the system. The electricity price refers to China's commercial average electricity price (0.8RMB/kWh).

The calculation results show that the SLHS system has good economic benefits. The system can achieve positive economic revenues within four years.

6. Conclusions

This paper presented the energy efficiency and optimum strategies for the operation of SLHS. The Energy Plus software was used to analyze the energy consumption of SLHS installed in a typical office building located in the city of Harbin. According to the validated hourly indoor illumination distribution throughout the year and the lighting design specification requirements, this study divided the offices into two lighting zones and developed an optimum lighting control strategy for SLHS. Main conclusions of this study are as follows:

(1) The simulation results showed that the overall energy consumption of lighting decreased by nearly 80% for office building. Which in return reduced the cooling load of the air-conditioning system during the summer by 4.49% due to lower generated heat from the lighting system inside the building.
(2) The SLHS provided supplementary natural light into the office which reduced the lighting energy consumption in the building. Due to the significant difference in light efficiency between natural light and LED lighting systems, for the same output illumination, the solar radiation energy required is much lower than the lighting electricity consumption. The analysis of the simulation demonstrated that comparing natural lighting with LED lighting systems, the required solar radiation energy is 39.4% lower than the required LED electricity power consumption.
(3) Based on the principle of SLHS, the energy saving benefit has been quantified based on the collector areas. For the collector area of 40 m^2, the energy saving rate of lighting and hot water systems are 58.9%, 19.3%, respectively. Through accounting, the SLHS can provide lighting demand of 30.46 m^2 of the building area and hot water demand of 9.92m^2 of the building area per square meter of the light-receiving area. At the same time, the SLHS can reduce the energy consumption of the air conditioner cooling load. The system can achieve positive economic revenues within four years. The above data are based on the annual average climate parameters. The system can achieve better productivity under the conditions of high direct sunlight and high outdoor dry bulb temperature.

7. Data availability statement

The data that support the findings of this study are available from the corresponding author upon reasonable request.

Declaration of Competing Interest

The authors declare that they have no known competing financial interests or personal relationships that could have appeared to influence the work reported in this paper.

CRediT authorship contribution statement

Chao Shen: Supervision, Writing – review & editing, Resources. **Kaijie Zheng:** Writing – original draft, Software, Formal analysis. **Changyun Ruan:** Validation, Formal analysis, Visualization. **Guoquan Lv:** Investigation, Data curation, Visualization.

Acknowledgement

The authors gratefully acknowledge the funding support from the Natural Science Foundation of Heilongjiang Province (No. YQ2020E019).

References

[1] Z.F. Liao, Z.Q. Liu, Q.Z. Wu, L. X.S, X.F. Zhan, G.R. Zeng, G.Q. Liu, Solar energy full-spectrum perfect absorption and efficient photo-thermal generation, Chin. Phys. B (08) (2021) 381–387.
[2] R. Liang, P. Wang, C. Zhou, Q. Pan, A. Riaz & J. Zhang, Thermal performance study of an active solar building faade with specific PV/T hybrid modules. Energy, 2020, 191.
[3] T.S. Kumar, S. Sharma, C.P. Kurian, et al., Adaptive neuro-fuzzy control of solar-powered building integrated with daylight-artificial light system, 2020 IEEE International Conference on Power Electronics, Smart Grid and Renewable Energy (PESGRE), IEEE, 2020.
[4] Nishchenko M.M., Chenko M.A., Tsapko E.A., et al., Hybrid system for solar energy conversion with nano-structured electrodes. 2020.
[5] N. Shishegar, M. Boubekri, E. Stine-Morrow, et al., Tuning environmental lighting improves objective and subjective sleep quality in older adults, Build. Environ. 204 (2) (2021) 108096.
[6] S. Ingimundardóttir, The influence of light and nature on health and well-being: a phenomenological study among a group of elderly in Iceland. Med. Health Sci., 2013.
[7] I.M. Iskra-Golec, A. Wazna, L. Smith, Effects of Blue-enriched Light on the daily course of mood, sleepiness and light perception: a field experiment, Soc. Light Light. 44 (4) (2012) 506–513.
[8] S.U.S. Choi, J.A. Eastman, in: Enhancing Thermal Conductivity of Fluids with Nanoparticles, 231, ASME-Publications-Fed, 1995, pp. 99–106.
[9] S.M. Wang, L.G. Hu, Z.D. Lu, D.M. Zhao, T.Z. Peng, Y.W. Zeng, D.R. Yang, Y. Zhao, J. Sha, J.J. Niu, White and bright radiation from nanostructured carbon, J. Optoelectron. Laser (2003).
[10] L.B. Mao, R.Y. Zhang, X.F. Ke, Z.J. Liu, Photo-thermal properties of nanofluid-based solar collector, Acta Energiae Solaris Sinca 30 (12) (2009) 1647–1652.
[11] J.F. Zhao, Study of Nanofluids' Radiation Properties and Its Utilization in Photovoltaic/Thermal System, Zhejiang University, 2009.
[12] A.W. Kandeal, Almoataz M. Algazzar, M.R. Elkadeem, Amrit Kumar Thakur, Gamal B. Abdelaziz, Emad M.S. El-Said, Ashraf Mimi Elsaid, Meng An, Reham Kandel, Hossam Eldin Fawzy, Swellam W. Sharshir, Nano-enhanced cooling techniques for photovoltaic panels: a systematic review and prospect recommendations, Sol. Energy, Volume 227, 2021, Pages 259–272.
[13] Ashraf Mimi Elsaid, Emad M.S. El-Said, Gamal B. Abdelaziz, Swellam W. Sharshir, Hamed R. El-Tahan, M.F. Abd Raboo, Performance and exergy analysis of different perforated rib designs of triple tubes heat exchanger employing hybrid nanofluids, Int. J. Therm. Sci. 168 (2021) 107006.
[14] F.A. Essa, Z.M. Omara, A.S. Abdullah, A.E. Kabeel, G.B. Abdelaziz, Enhancing the solar still performance via rotating wick belt and quantum dots nanofluid, Case Stud. Therm. Eng. 27 (2021) 101222.
[15] Gamal B. Abdelaziz, Almoataz M. Algazzar, Emad M.S. El-Said, Ashraf Mimi Elsaid, Swellam W. Sharshir, A.E. Kabeel, S.M. El-Behery, Performance enhancement of tubular solar still using nano-enhanced energy storage material integrated with v-corrugated aluminum basin, wick, and nanofluid, J. Energy Storage 41 (2021) 102933.
[16] Swellam W. Sharshir, Mohamed A. Hamada, A.W. Kandeal, Emad M.S. El-Said, Ashraf Mimi Elsaid, Maher Rashad, Gamal B. Abdelaziz, Augmented performance of tubular solar still integrated with cost-effective nano-based mushrooms, Sol. Energy, Volume 228, 2021, Pages 27–37.
[17] Swellam W. Sharshir, A.W. Kandeal, M. Ismail, Gamal B. Abdelaziz, A.E. Kabeel, Nuo Yang, Augmentation of a pyramid solar still performance using evacuated tubes and nanofluid: experimental approach, Appl. Therm. Eng. 160 (2019) 113997.
[18] Tielke J., Maas M., Castillo M., Rezwan K., & Avila M., Statistical analysis of thermal conductivity experimentally measured in water-based nanofluids. 2021.
[19] E. Torres, I. Carrillo-Berdugo, D. Zorrilla, J. Sánchez-Márquez, J. Navas, CuO-containing oil-based nanofluids for concentrating solar power: an experimental and computational integrated insight, J. Mol. Liq. 325 (2020) 114643.
[20] Q. Qiao, A. Yunusa-Kaltungo, R.E. Edwards, Towards developing a systematic knowledge trend for building energy consumption prediction, J. Build. Eng. (April 2020) 101967.
[21] K. Rajeev, M. Francesca, W. Chatura, N. Arunkumar, D.Y. Goswami, Strategic control and cost optimization of thermal energy storage in buildings using energy plus, Appl. Energy 246 (JUL.15) (2019) 77–90.
[22] Gamal B. Abdelaziz, M.A. Abdelbaky, M.A. Halim, M.E. Omara, I.A. Elkhaldy, A.S. Abdullah, Z.M. Omara, F.A. Essa, Aml Ali, Swellam W. Sharshir, Emad M.S. El–Said, Ahmed G. Bedair, A.E. Kabeel, Energy saving via heat pipe heat exchanger in air conditioning applications "experimental study and economic analysis, J. Build. Eng. 35 (2021) 102053.
[23] C. Shen, G.Q. Lv, K.J. Zheng, C.Y. Ruan, C.X. Zhang, Y. Dong, Modeling and investigating the detailed characteristics of solar lighting/heating system based on spectrum split of nanofluids, Energy Built Environ. (2020).
[24] L. Li, Optimization and Experimental Study of Optical Fiber Transmission Day Lighting System, North China Electric Power University (Beijing, 2019.
[25] I.M. Kirpichnikova, O.S. Volkova, A.A. Maliugina, Using solar optical fibers for public buildings illumination in the south Urals, Procedia. Eng. 129 (2015) 195–200.
[26] W. Chen, H. Abdul-Rahman, S.P. Rao, Daylighting can be fluorescent: development of a fiber solar concentrator and test for its indoor illumination, Energy Build. 42 (2010) 717–727.
[27] C. Kandilli, K. Ulgen, Review and modelling the systems of transmission concentrated solar energy via optical fibers, Renew. Sustain. Energy Rev. 13 (2009) 67–84.
[28] JGJ 26-2010, Design standard for energy efficiency of residential buildings in severe cold and cold zones, 2010.
[29] C.F. Zhang, Study On The Law of the Heating Room Indoor Diurnal Temperature Changing in the Frore Region, Daqing Petroleum Institute, 2008.
[30] C.P. Wu, J.H. Peng, H. Jiang, Numerical analysis of heat-insulating property of walls with different structures, Gas Heat 31 (11) (2011) 27–32.
[31] Y. Dong, X.R. Xu, J.Q. Bai, Heating season thermal load analysis of Beijing residential building based on DEST simulation, District Heat. 2019(03):32–37.
[32] Y.N. Ping, Study On Interior Illuminance Control System Based on Daylighting, Zhengzhou University, 2012.
[33] J.Q. Li, Constant Illumination Control Strategy Research Combined Natural Lighting with Intelligent Lighting, Zhengzhou University of Light Industry, 2019.
[34] G.W. Li, Architectural Lighting Design Manual, China Architecture & Building Press, 2004.
[35] C. Shen, G.Q. Lv, S. Wei, C.X. Zhang, C.Y. Ruan, Investigating the performance of a novel solar lighting/heating system using spectrum-sensitive nanofluids, Appl. Energy 270 (2020) 115208.
[36] H.D. Behr, Solar radiation on tilted south oriented surfaces: validation of transfer–models, Sol. Energy 61 (6) (1998) 399–413.
[37] J.R. Coaton, A.M. Marsden, Lamps and Lighting, Fudan University Press, 2000.